

~~CONFIDENTIAL~~Copy 5  
RM L52L02

JUL 3 1953

UNCLASSIFIED

  
NACA

## RESEARCH MEMORANDUM

A COMPARISON OF GUST LOADS MEASURED IN FLIGHT  
ON A SWEEP-WING AIRPLANE AND AN  
UNSWEPT-WING AIRPLANE

By Jack Funk and Harry C. Mickleboro

Langley Aeronautical Laboratory  
Langley Field, Va.

CLASSIFICATION CANCELLED

Auth. *NACA R92772* Date *10/12/54*By *mdt* *11/9/54* See \_\_\_\_\_

CLASSIFIED DOCUMENT

This material contains information affecting the National Defense of the United States within the meaning of the espionage laws, Title 18, U.S.C., Secs. 793 and 794, the transmission or revelation of which in any manner to an unauthorized person is prohibited by law.

NATIONAL ADVISORY COMMITTEE  
FOR AERONAUTICS

WASHINGTON

June 29, 1953

UNCLASSIFIED

~~CONFIDENTIAL~~

NACA LIBRARY

LANGLEY AERONAUTICAL LABORATORY  
Langley Field, Va.

NACA RM L52L02

~~CONFIDENTIAL~~

UNCLASSIFIED

## NATIONAL ADVISORY COMMITTEE FOR AERONAUTICS

## RESEARCH MEMORANDUM

A COMPARISON OF GUST LOADS MEASURED IN FLIGHT  
ON A SWEEP-WING AIRPLANE AND AN  
UNSWEPT-WING AIRPLANE

By Jack Funk and Harry C. Mickleboro

## SUMMARY

Flight tests were conducted with two jet-propelled airplanes in rough air to investigate effects of sweep on gust loads and gust selectivity. Data were obtained with an unswept-wing airplane and a  $35^\circ$  swept-wing airplane for incremental accelerations up to 0.7 and 1.1 g corresponding to airspeeds of 300 and 450 miles per hour, respectively. The ratio of the loads on the swept-wing airplane to those on the unswept-wing airplane was 0.82 for both test speeds. Simple analysis and previous gust-tunnel investigations had indicated that the loads ratio should be nearly proportional to the ratio of the slopes of the lift curves. The experimental loads ratio agreed well with the ratio of the lift-curve slopes obtained from low-speed wind-tunnel tests or calculated by the

empirical relation  $a = \frac{6A \cos \Lambda}{A + 2 \cos^2 \Lambda}$ , where  $a$  is the slope of the lift

curve,  $A$  is the aspect ratio, and  $\Lambda$  is the angle of sweep. The loads ratio also agreed closely with the cosine of the angle of sweep, indicating that, for wings of moderate aspect ratio, the cosine of the sweep angle would approximate the reduction of gust loads that could be expected because of sweep. An analysis of the gust gradient distances indicated only slight differences in the gust selectivity characteristics of the two airplanes.

## INTRODUCTION

The aerodynamic loads imposed by flight through turbulent air are frequently the critical loads in the design of transport and bomber airplanes. Most gust-load studies made in the past were confined to unswept wings but the increasing use of swept wings has created a need for information on the effect of sweep on gust loads. Various factors which are known to affect the gust loads on swept wings are lift-curve slope, gust

~~CONFIDENTIAL~~

UNCLASSIFIED

selectivity, stability, and rate of penetration into the gust. The gust selectivity of the airplane is defined as that portion of the gust spectrum which causes aerodynamic loads above a specified threshold.

Some information has been obtained concerning the over-all effects of sweep on gust loads from gust-tunnel tests (refs. 1, 2, and 3) in which the swept wings were derived from the unswept wings by rotation. The results of these tests indicate that for a single gust the gust loads on swept wings as compared to the gust loads on the corresponding unswept wings are roughly proportional to the ratio of the lift-curve slopes with a small reduction due to penetration effects. The gust-tunnel tests, however, are restricted to small-scale models and to the simplified representation of atmospheric turbulence by a single gust. Moreover, the gust tunnel provides little or no information concerning the gust selectivity between different wing configurations. A flight investigation of the effect of sweep on gust loads was needed, therefore, to provide some data for correlation with the gust-tunnel work and to determine the gust selectivity of the swept-wing airplane.

A cooperative flight investigation was undertaken by the National Advisory Committee for Aeronautics and the Directorate of Flight and All-Weather Testing, Wright Air Development Center, Air Research and Development Command, U. S. Air Force. A swept-wing airplane and an unswept-wing airplane, which were roughly similar except for sweep, were utilized. The airplanes were jet fighters supplied by the U. S. Air Force. Side-by-side flights (similar to those of ref. 4) were made in turbulent air to obtain a comparison of the gust loads and gust selectivity of the two airplanes. This report presents an analysis of the results obtained from this phase of the flight tests.

#### APPARATUS AND TESTS

Two jet-propelled airplanes, one with unswept wings and one with the wings swept back  $35^\circ$ , were used in the investigation. Three-view drawings of the two test airplanes are shown in figure 1. The pertinent characteristics of each airplane as flown are given in table I. Also included in table I are values of an equivalent unswept-wing derived by rotation of the swept wing about its  $\frac{1}{4}$ -chord point to an angle of zero sweep. A comparison of the characteristics of the equivalent unswept-wing airplane to those of the unswept-wing airplane used in the tests indicates that the test airplanes approximated the condition of an unswept wing and a swept wing obtained by rotation of the  $\frac{1}{4}$ -chord line of the unswept wing.

The following instruments were installed in each airplane to obtain information pertinent to the gust loads:

- (1) NACA magnetically damped recording accelerometer
- (2) NACA airspeed-altitude recorder
- (3) NACA 1-second interval timer

The recording accelerometers were damped to 0.7 of critical and had a natural vane frequency of about 19 cycles per second. Their range for a full-scale film deflection of 2 inches was from -1 g to 3g. The accelerometers were located as near as practicable to the center of gravity of each airplane. For the unswept-wing airplane, the accelerometer was located approximately 5.5 feet forward of the normal center of gravity of the airplane. In the swept-wing airplane the accelerometer was mounted approximately 2.3 feet forward of the normal center of gravity of the airplane. Corrections to the measured accelerations due to displacement of the recording instrument from the center of gravity will be discussed subsequently.

The static-pressure source for the recording airspeed installation of each airplane was calibrated by the fly-by method (ref. 5), and the results are given in figure 2 where the static-pressure error is shown as a function of the indicated Mach number.

The test procedure consisted of 12 side-by-side flights through clear air turbulence over a fixed course of about 22 miles in the vicinity of Dayton, Ohio. All flights were made in continuous rough air at an altitude of approximately 1500 feet above terrain. Each flight consisted of four runs, two at 300 miles per hour and two at 450 miles per hour. The pilots' assignments and the order of the high- and low-speed runs were varied randomly to eliminate any consistent combination of conditions that might affect the results. A minimum of pilot control was used on all flights. No external tanks were used on either airplane and the dive brakes remained closed throughout the tests.

#### EVALUATION AND RESULTS

The acceleration records were evaluated to obtain the maximum value of acceleration between any two consecutive intersections of the record line with the 1 g reference and the distance traveled from each intersection to the following peak acceleration. The latter measurement is considered a measure of the gust gradient distance and is referred to as such in this report. The evaluation was confined to values of acceleration increment greater than 0.3g and 0.45g for the low- and high-speed runs of the unswept-wing airplane, and 0.25g and 0.35g for the swept-wing airplane. These thresholds correspond to effective gust velocities of approximately 5 feet per second.

The airspeed-altitude records were evaluated to obtain an average airspeed and altitude for each run and the total flight distance in air miles of each run. Corrections were made for static-pressure errors according to the calibration shown in figure 2.

Since the recording accelerometers of both airplanes were not located exactly at the center of gravity, it was necessary to correct the measured accelerations for the angular acceleration of the airplane. The corrections were made by use of the following equation which is equation (A6) from appendix A of reference 4:

$$\Delta n_{cg} = \frac{\Delta n_A}{1 + \frac{W}{I_y g}(X^2 - BX)}$$

where

$\Delta n_{cg}$	acceleration increment at center of gravity
$\Delta n_A$	measured acceleration increment
$W$	airplane weight
$I_y$	pitching moment of inertia of airplane about center of gravity
$g$	acceleration of gravity
$X$	distance from center of gravity to recording accelerometer
$B$	distance from recording accelerometer to center of lift

This equation takes into account the effect of pitching motion on acceleration measurements made away from the center of gravity of the airplane and has been shown to agree very well with flight results. The acceleration correction amounted to 4 percent for the unswept-wing airplane and  $5\frac{1}{2}$  percent for the swept-wing airplane. The acceleration data for both airplanes were further corrected to a standard condition (wing loading of 45 pounds per square foot and a forward velocity of 300 or 450 miles per hour) on the basis of the assumption that the acceleration increment varies directly as the forward speed and inversely as the wing loading. The correction was made to eliminate any effects resulting from small variations in these quantities which occurred from run to run.

The corrected acceleration data were sorted into frequency distributions with class intervals of 0.05g. These data are tabulated in

table II with the total flight miles for each test condition. The cumulative frequency distribution, obtained by successive addition of the frequencies of table II, were divided into the total flight miles to obtain the average number of miles flown to equal or exceed a given acceleration. These results are shown plotted in figure 3. As a comparison of the gust loads experienced by the two airplanes, the ratios of the gust loads on the swept-wing airplane to the gust loads on the unswept-wing airplane were obtained for equal flight distances from figure 3. The load ratios are shown in figure 4 as a function of various acceleration increments of the unswept-wing airplane. The loads ratios are shown in figure 4 only for acceleration increments up to 0.66g for the tests at 300 miles per hour and 1.00g for the tests at 450 miles per hour because of the small sample size for higher acceleration increments.

Considering the scatter of the data, reading accuracies, and consistency of repeated runs, the over-all precision of the load ratios as determined from the flight data is estimated to be within  $\pm 3$  percent.

The gradient distances for all accelerations corresponding to effective gust velocities of approximately 6 feet per second or higher were sorted into class intervals of 5 chords from which relative frequency distributions were obtained. Figure 5 presents the distributions for the gradient distances measured in mean aerodynamic chords (streamwise chords) for both airplanes. Also included in figure 5 is a distribution of gradient distances for the swept-wing airplane measured in panel chords (mean aerodynamic chords multiplied by the cosine of the sweep angle).

#### DISCUSSION

From figure 3 it can be seen that, for an equal number of miles flown at each speed, the swept-wing airplane experienced lower loads in turbulent air than the unswept-wing airplane. The average ratio of loads on the swept-wing airplane to the loads on the unswept-wing airplane, shown in figure 4, is approximately 0.82 for both test speeds and is fairly constant throughout the acceleration range covered by the tests.

The effect of sweep on the gust selectivity of the two airplanes involved in this investigation may be seen from a study of figure 5, which presents the frequency distribution of gust gradient distances for both airplanes. It is seen from the figure that there is little difference in the gust selectivity for the swept- and the unswept-wing airplanes. Based on streamwise chords, the gust gradient distance most frequently experienced was 13 chords for the unswept-wing airplane and 15 chords for the swept-wing airplane. Figure 5 also presents the distribution of gust gradient distances on the basis of panel chords, for the swept-wing airplane only. This distribution agrees rather closely in both magnitude and shape with that, based on the streamwise chord, for the unswept-wing airplane.

Calculations of the gust-loads ratio can be made by using the sharp-edge-gust equation and the acceleration ratio

$$\Delta n = \frac{\rho S U a}{2W} \frac{\Delta n}{\Delta n_s}$$

where

$\Delta n$  acceleration increment

$\rho$  air density

$S$  wing area

$U$  gust velocity

$V$  forward velocity

$a$  slope of lift curve

$W$  airplane weight

$\frac{\Delta n}{\Delta n_s}$  acceleration ratio

$\Delta n_s$  acceleration increment due to sharp-edge gust,  $\frac{\rho S U a}{2W}$

Since the acceleration data were corrected for wing loading and speed differences and since the airplanes were flown at the same altitude, the loads ratio for the two airplanes reduces to

$$\frac{\Delta n_1}{\Delta n_2} = \frac{a_1}{a_2} \frac{(\Delta n / \Delta n_s)_1}{(\Delta n / \Delta n_s)_2}$$

where subscripts 1 and 2 refer to the swept- and unswept-wing airplanes, respectively. The loads ratio may be defined in terms of a single parameter, the ratio of the lift-curve slopes, if the acceleration ratios are equal for both airplanes. The primary variables affecting the acceleration ratio are mass ratio and gust selectivity with some effect due to the gradual penetration of the swept wing into the gust. From table I and figure 5 it is noted that the mass ratios and gust selectivities of the two airplanes are nearly the same. Gust-tunnel tests and calculations indicate that the effect of penetration would be less than 2 or 3 percent for sweep angles up to  $45^\circ$ . It appears, therefore, that only small errors are introduced in this case by assuming that the acceleration ratios for the two airplanes are equal.

The following table compares experimental loads ratio with the ratio of the lift-curve slopes of the two airplanes obtained from several

sources, where  $M$  is the Mach number and  $A$  is the aspect ratio. Values of the wind-tunnel lift-curve slopes were taken from reference 6 and unpublished data and reproduced herein as figure 6.

Loads ratio obtained from flight tests	
at $M = 0.4$ and $0.6$ . . . . .	0.82
Ratio of wind-tunnel lift-curve slopes:	
at $M = 0.4$ . . . . .	0.81
at $M = 0.6$ . . . . .	0.78
Ratio of lift-curve slopes based on	
$\frac{6A \cos \Lambda}{A + 2 \cos^2 \Lambda}$ . . . . .	0.84
$\cos \Lambda$ . . . . .	0.82

It may be noted from this table that the load ratios based on the cosine of sweep, the empirical formula, and the wind-tunnel lift-curve slopes of  $M = 0.4$  are in good agreement with the flight tests. The agreement between the loads ratio and the cosine of the sweep angle indicates that the latter may be used as a rough estimate for determining the reduction in loads that might be expected because of sweep. This relation would not be expected to apply at very low aspect ratios or at very high angles of sweep. The load ratio obtained from the wind-tunnel lift-curve slope at  $M = 0.6$  does not agree with the flight tests and is not within the experimental error of the tests. This may have been expected on the basis of reference 7 where it was shown that no Mach number correction was needed for lift-curve slopes used for the prediction of gust loads on unswept wings, even though such a correction appeared valid from wind-tunnel tests.

#### CONCLUDING REMARKS

Results of a flight investigation of two jet-propelled airplanes to determine the effect of sweep on gust loads and gust selectivity show that the  $35^\circ$  swept-wing airplane experienced lower loads in turbulent air than the unswept-wing airplane. As indicated by previous gust-tunnel investigations of sweep, the ratio of loads on the two airplanes agreed well with the ratio of the lift-curve slopes related by the cosine of the sweep angle or calculated by the empirical formula  $\frac{6A \cos \Lambda}{A + 2 \cos^2 \Lambda}$ , where  $A$  is the aspect ratio and  $\Lambda$  is the angle of sweep. The experimental loads ratio also agreed with the ratio of lift-curve slopes from low-speed wind-tunnel data, but the use of high-speed wind-tunnel data



does not lead to as good agreement. An analysis of the gust gradient distances indicated only slight differences in the gust selectivity characteristics of the two airplanes.

Langley Aeronautical Laboratory,  
National Advisory Committee for Aeronautics,  
Langley Field, Va.

#### REFERENCES

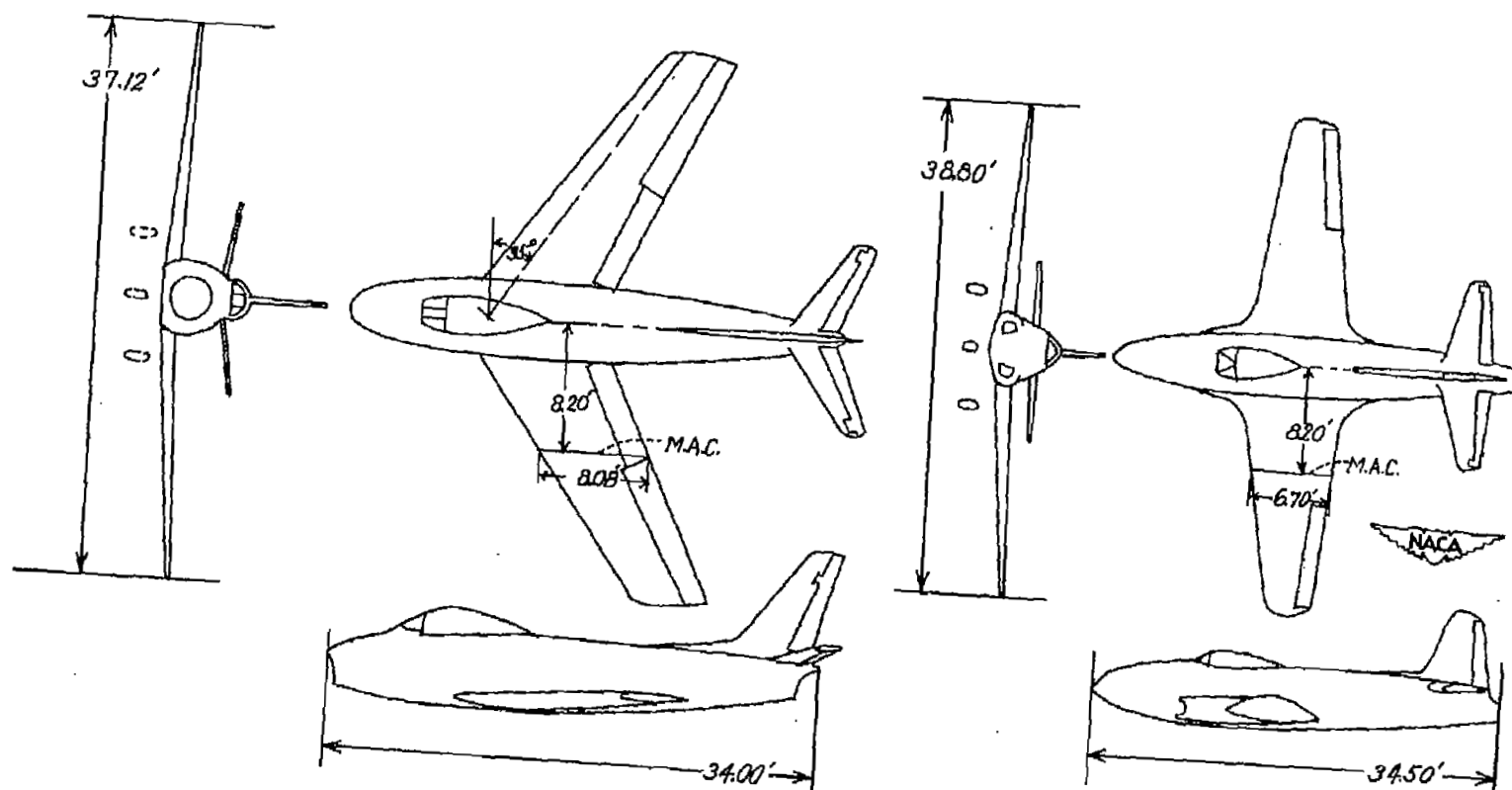
1. Reisert, Thomas D.: Gust-Tunnel Investigation of a Wing Model With Semichord Line Swept Back  $30^{\circ}$ . NACA TN 1794, 1949.
2. Pierce, Harold B.: Tests of a  $45^{\circ}$  Sweptback-Wing Model in the Langley Gust Tunnel. NACA TN 1528, 1948.
3. Pierce, Harold B.: Gust Tunnel Investigation of a Wing Model With Semichord Line Swept Back  $60^{\circ}$ . NACA TN 2204, 1950.
4. Funk, Jack, and Binckley, Earle T.: A Flight Investigation of the Effect of Center-of-Gravity Location on Gust Loads. NACA TN 2575, 1951.
5. Thompson, F. L., and Zalovcik, John A.: Airspeed Measurements in Flight at High Speeds. NACA ARR, Oct. 1942.
6. Triplett, William C., and Van Dyke, Rudolph D., Jr.: Preliminary Flight Investigation of the Dynamic Longitudinal-Stability Characteristics of a  $35^{\circ}$  Swept-Wing Airplane. NACA RM A50J09a, 1950.
7. Binckley, E. T., and Funk, Jack: A Flight Investigation of the Effects of Compressibility on Applied Gust Loads. NACA TN 1937, 1949.

TABLE I  
AIRPLANE CHARACTERISTICS

Item	Unswpt-wing airplane	35° swept-wing airplane	Equivalent unswpt wing
Mean aerodynamic chord, $c$ , ft . . . . .	6.7	8.08	6.62
Slope of lift curve for zero Mach number, $a$ , per radian (ref. 6 and unpublished data) . . .	4.7	3.8	4.64
Wing area, $S$ , sq ft . . . . .	237	288	288
Average test weight, $W$ , lb.	10,870	12,820	12,820
Average wing loading, $W/S$ , lb/sq ft . . . . .	45.9	44.5	44.5
Wing span, ft . . . . .	38.9	37.1	45.3
Aspect ratio, $A$ . . . . .	6.39	4.79	7.15
Center-of-gravity location, percent M.A.C. . . . .	28.4	22.0	----
Sweep angle of quarter chord, $\Lambda$ , deg . . . . .	5	35	0
Moment of inertia, $I_y$ , slug-ft <sup>2</sup> . . . . .	15,000	17,480	----
Av. mass ratio, $\frac{2 W/S}{\rho g c a}$ . .	40.7	40.6	40.6
Slope of lift curve from $\frac{6A \cos \Lambda}{A + 2 \cos^2 \Lambda}$ , per radian . .	4.56	3.84	4.68

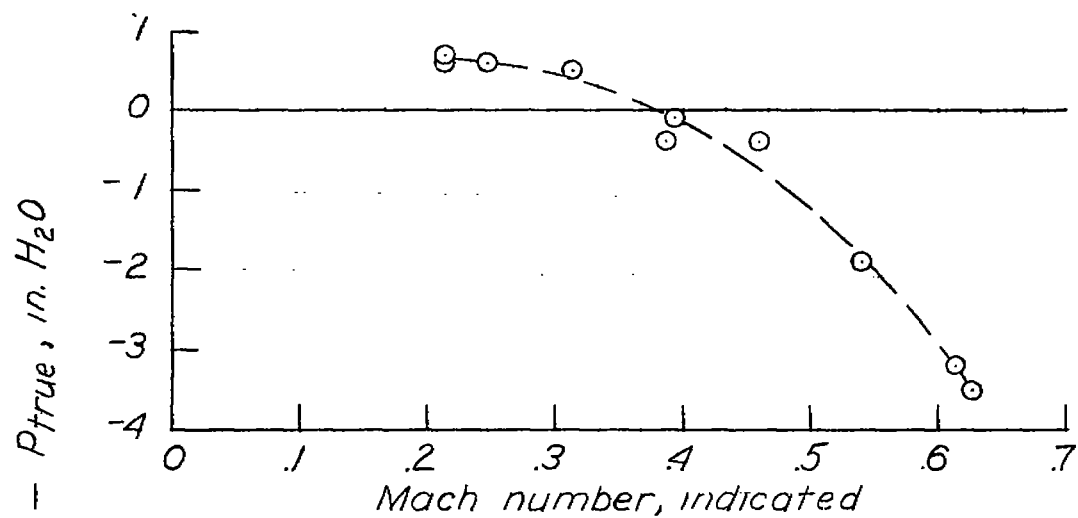
TABLE II  
FREQUENCY DISTRIBUTION OF ACCELERATION

Number of Acceleration Increments		
Class interval, $\Delta n$ , g	Unswept-wing airplane	Swept-wing airplane
V = 300 MPH		
0.20 to 0.25	---	---
.25 to .30	---	477
.30 to .35	284	225
.35 to .40	249	116
.40 to .45	127	52
.45 to .50	80	23
.50 to .55	38	13
.55 to .60	25	2
.60 to .65	12	2
.65 to .70	8	2
.70 to .75	3	3
.75 to .80	1	0
Total flight miles	522.6	517.4
V = 450 MPH		
0.35 to 0.40	---	399
.40 to .45	---	270
.45 to .50	308	176
.50 to .55	194	118
.55 to .60	135	62
.60 to .65	114	37
.65 to .70	77	28
.70 to .75	42	12
.75 to .80	29	8
.80 to .85	20	8
.85 to .90	15	4
.90 to .95	11	0
.95 to 1.00	8	1
1.00 to 1.05	6	2
1.05 to 1.10	2	1
1.10 to 1.15	2	2
1.15 to 1.20	3	0
Total flight miles	522.9	523.7

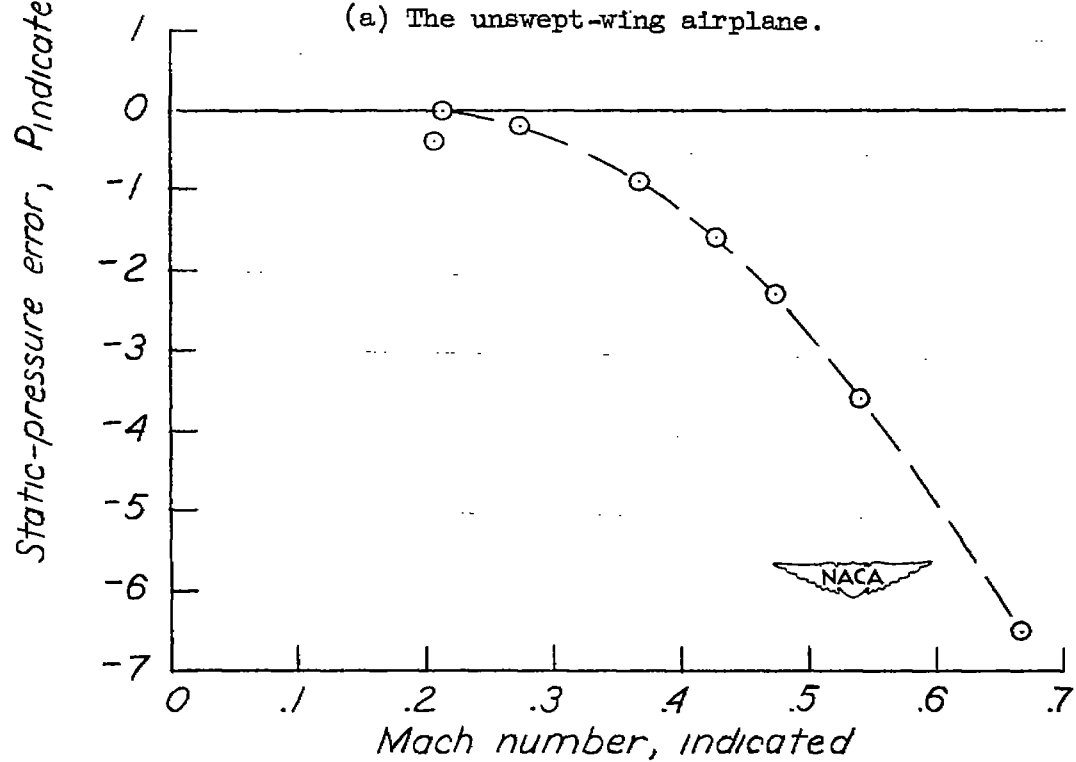


(a) The 35° swept-wing airplane. (b) The unswept-wing airplane.

Figure 1.- Three-view drawing of test airplanes.



(a) The unswept-wing airplane.



(b) The swept-wing airplane.

Figure 2.- Static-pressure-source calibration of test airplanes by fly-by method.

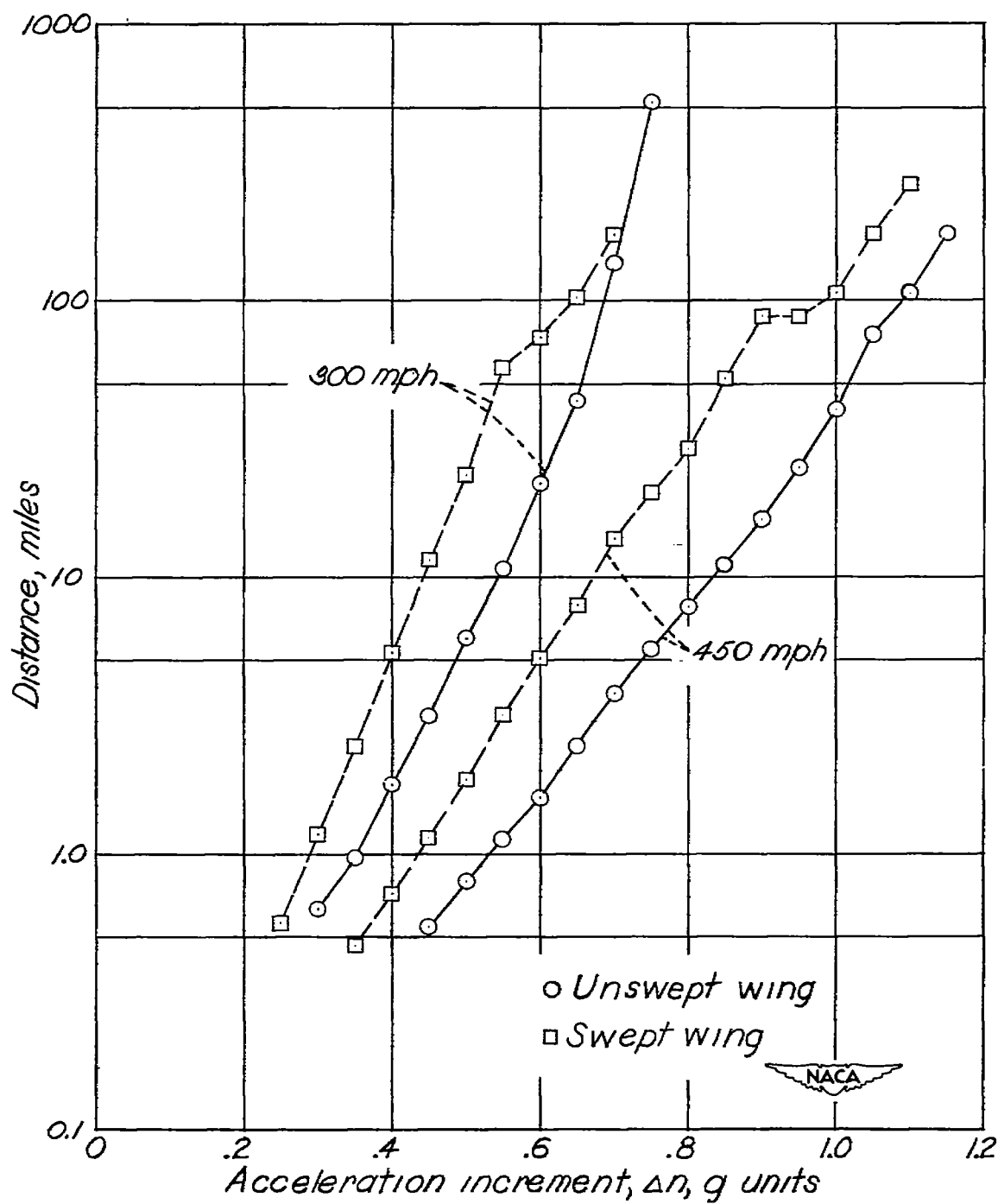


Figure 3.- Average number of miles flown to exceed a given acceleration increment.

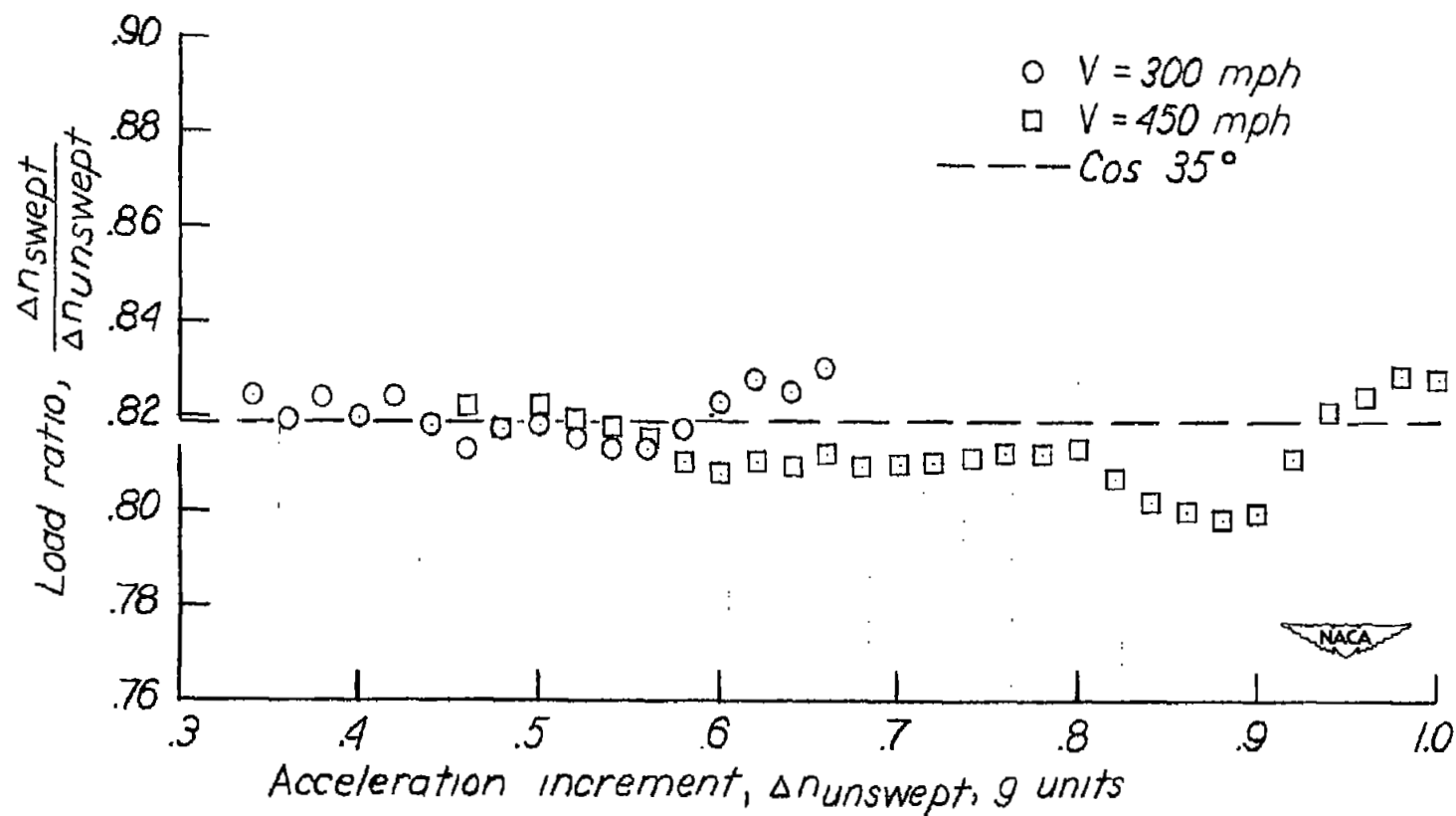


Figure 4.- Ratio of gust loads on a swept and unswept wing.

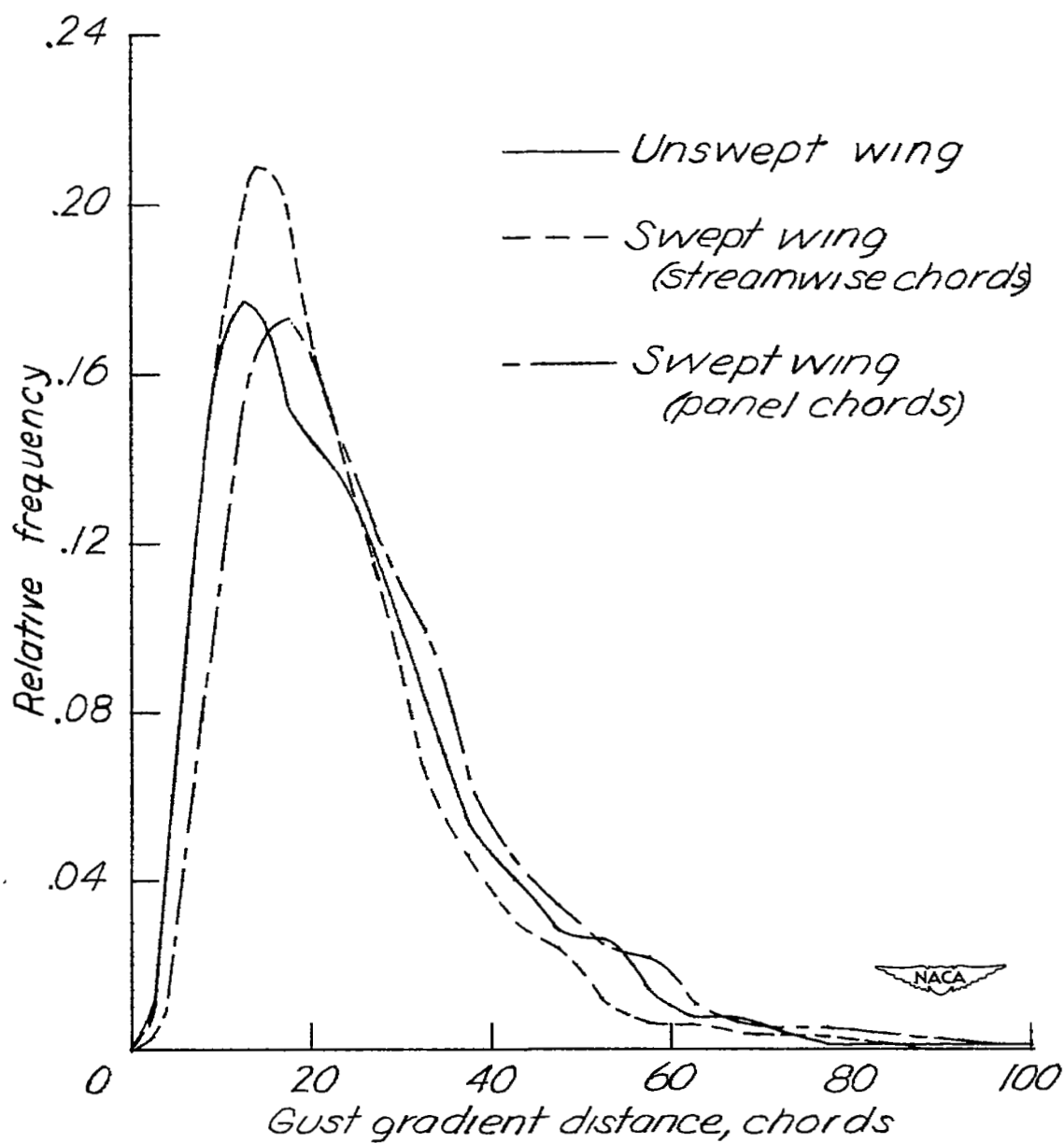


Figure 5.- Frequency distribution of gust gradient distances.



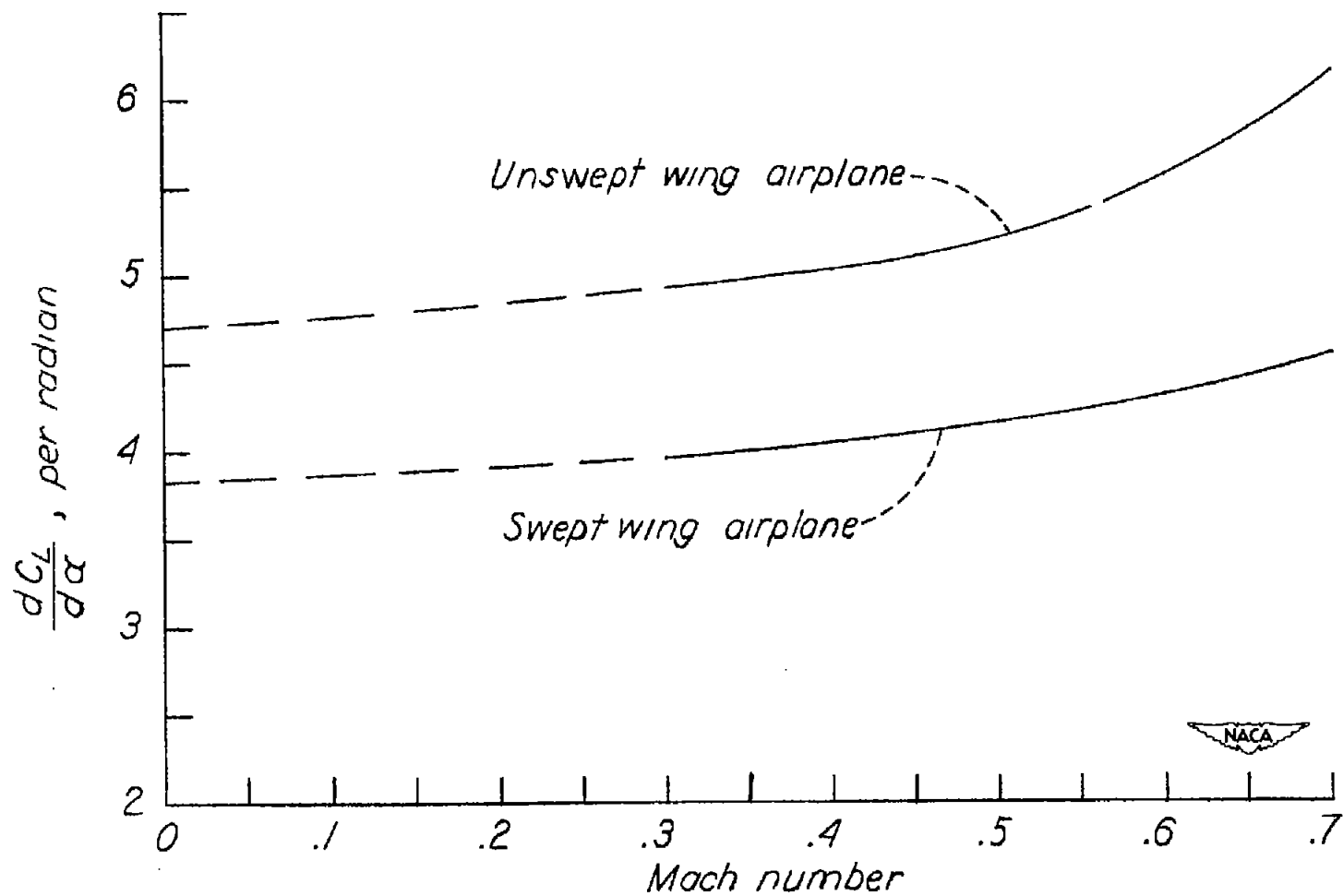


Figure 6.- Wind-tunnel lift-curve slopes of test airplanes (ref. 6 and unpublished data).